Reactive scattering of H2 from Cu(100): six-dimensional quantum dynamics results for reaction and scattering obtained with a new, accurately fitted potential-energy surface

Somers, M.F.; Olsen, R.A.; Busnengo, H.F.; Baerends, E.J.; Kroes, G.

published in
Journal of Chemical Physics
2004

DOI (link to publisher)
10.1063/1.1812743

document version
Publisher's PDF, also known as Version of record

Reactive scattering of H_2 from Cu(100): Six-dimensional quantum dynamics results for reaction and scattering obtained with a new, accurately fitted potential-energy surface

M. F. Somers and R. A. Olsen
Leiden Institute of Chemistry, Gorlaeus Laboratories, Leiden University, P.O. Box 9502, 2300 RA, Leiden, The Netherlands

H. F. Busnengo
Instituto de Física Rosario (Consejo de Investigaciones Cientificas–Universidad Nacional de Rosario) and Facultad de Ciencas Exactas, Ingeniería y Agrimensura, Universidad Nacional de Rosario, Avenida, Pellegrini 250, 2000 Rosario, Argentina

E. J. Baerends
Theoretical Chemistry, Free University, De Boelelaan 1083, 1081 HV Amsterdam, The Netherlands

G. J. Kroes[a)]
Leiden Institute of Chemistry, Gorlaeus Laboratories, Leiden University, P.O. Box 9502, 2300 RA, Leiden, The Netherlands

(Received 24 May 2004; accepted 14 September 2004)

Six-dimensional quantum dynamical calculations are reported for the dissociative chemisorption of ($v=0$, 1, $j=0$) H_2 on Cu(100), and for rovibrationally inelastic scattering of ($v=1$, $j=1$) H_2 from Cu(100). The dynamics results were obtained using a new potential-energy surface (PES5), which was based on density-functional calculations using a slab representation of the adsorbate-substrate system and a generalized gradient approximation to the exchange-correlation energy. A very accurate method (the corrugation reducing procedure) was used to represent the density-functional theory data in a global potential-energy surface. With the new, more accurately fitted PES5, the agreement between the dynamics results and experimental results for reaction and rovibrationally elastic scattering is not as good as was obtained with a previous potential-energy surface (PES4), which was based on a subset of the density-functional theory data not yet including the results for the low-symmetry Cu sites. Preliminary density-functional theory results suggest that the agreement between theory and experiment will improve over that obtained with PES5 if the density-functional calculations are repeated using a larger basis set and using more copper layers than employed in PES4 and PES5. © *2004 American Institute of Physics.* [DOI: 10.1063/1.1812743]

I. INTRODUCTION

Experimentally, H_2+metal surface systems are the best characterized systems consisting of a molecule interacting with a metal surface. Molecular-beam experiments have measured the dissociative chemisorption probability of H_2 (or D_2) as a function of the collision energy (E_i) for many metal surfaces.[1–8] From such experiments, reaction probabilities resolved with respect to the initial vibrational state[1–4] or the initial rotational state[8] have been obtained using seeded beam techniques for a number of systems. Information on the simultaneous effect on the reaction of the initial quantum numbers for the vibration (v) and the angular momentum (j) of the molecule,[1–3] and even on the effect of the rotational quadrupole alignment of the incoming molecule,[9,10] was obtained using associative desorption experiments, assuming a detailed balance. Molecular-beam experiments have further provided information on vibrationally inelastic scattering[11,12] and rotationally (in)elastic scattering,[13,14] in some cases obtaining state-to-state results for transitions in which both v and j undergo changes.[15,16]

Theoretically, it has now been established that six-dimensional (6D) quantum dynamics calculations can yield accurate results for the dissociative chemisorption of H_2 on metal surfaces,[17] if based on potential-energy surfaces (PESs) computed using density-functional theory (DFT).[18–23] In these dynamics calculations, the six molecular degrees of freedom are treated essentially without approximations, and the DFT calculation of the PES is done within the generalized gradient approximation (GGA)[24–26] and employing a periodic representation of the adsorbate-substrate system.[27,28] In the model, electron-hole pair excitations and phonon-inelastic scattering are neglected, based on the assumptions discussed in Refs. 29–31.

Remarkably and maybe even fortuitously good agreement of theory with experiment has been obtained for dissociative chemisorption, using the model outlined above for the H_2+Cu(100),[21] H_2+Pt(111),[32] H_2+Pd(100),[33] and H_2+Pd(111) (Ref. 34) systems. For these systems, the good agreement with experiment obtained for H_2+Pt(111) and H_2+Pd(111) is perhaps most significant, the dynamics cal-

[a)]Electronic mail: g.j.kroes@chem.leidenuniv.nl

culations being based on accurate interpolations of well-converged DFT data. In particular, the highly accurate corrugation reducing procedure (CRP) method[35] was used to represent the DFT data in a global PES[36,37] in both cases. With this method, the difference between the fit and the DFT data not used to obtain the fit was less than 30 meV in the entrance and barrier regions of the PES, for both systems. The DFT data for $H_2+Pt(111)$ were obtained in calculations using a basis set of almost double zeta+one polarization function quality and used three metal layers to model the surface.[22] The DFT data for $H_2+Pd(111)$, which were converged to within better than 0.1 eV as was the case for the $H_2+Pt(111)$ data, were obtained in calculations using five metal layers to model the surface.[23,37] In contrast to the favorable comparisons obtained between theory and experiment for reaction, comparisons of quantum dynamics and experimental results for $H_2+Cu(100)$ (Ref. 16) and HD $+Pt(111)$ (Ref. 38) for state-to-state rovibrationally inelastic scattering show that it is much harder to accurately describe the latter process using the model outlined above.

The dissociative chemisorption of H_2 on Cu(100)—the system we focus on here—has been studied in molecular-beam[5] and in associative desorption[39] experiments, and the results of these experiments have been fitted to reaction probability curves describing the dependence of the dissociation of (v) H_2 on E_i for $v=0$ and 1.[40] In addition, rovibrationally elastic and inelastic scattering of $(v=1,\ j=1)$ H_2 from Cu(100) has been studied by Watts *et al.*[16] Previous 6D quantum dynamics calculations for $H_2+Cu(100)$ gave good agreement with the experiment for reaction,[21] and for rovibrationally elastic scattering of $(v=1,\ j=1)$ H_2.[16] However, the same calculations employing the same PES (PES4)[21] overestimated the probabilities for rotational excitation (from $v=1,\ j=1$ to $v=1,\ j=3$) and for vibrationally and rotationally inelastic scattering (to $v=0$ and $j=5,\ 7$) by about a factor of 5.[16] The theorists, in the paper describing these results, speculated that the overestimation of the latter processes could be due to the use of an imperfect fitting method to represent the DFT data, in PES4. The anisotropy of the molecule-surface interaction was described using spherical harmonics (for the H_2 rotation) up to fourth order only, and it was speculated that this could lead to a too large anisotropy of PES4, which would then lead to too much rotationally inelastic scattering.

One goal of this paper is to assess whether more accurate results for (vibrationally and) rotationally inelastic scattering of H_2 from Cu(100) can be obtained using a much more accurately fitted PES (PES5),[36] employing the CRP method.[35] The new PES correctly describes the effect that, if the molecule is not parallel to the surface, the molecule-surface interaction changes if the molecule is rotated by an angle of 180° in the azimuthal angle ϕ above low-symmetry sites, as discussed below. This effect was not yet correctly described by PES4. More generally, the CRP method should provide a much more accurate description of the anisotropy and corrugation of the molecule-surface interaction than realized in PES4. PES5 is based on the DFT data obtained using the same DFT-parameter settings as used before to obtain PES4. An advantage of this approach is that the importance of using a very accurate fitting method, which correctly describes the interaction of the molecule also above low-symmetry sites, can be assessed by comparison of the dynamics results to those obtained using a less accurate fitting method but based on DFT data of the same quality.

More generally, the goal of this paper is to provide the definitive comparison between theory and experiment for the reaction of H_2 on and the rovibrationally (in)elastic scattering of H_2 from Cu(100) for the DFT model[21] that we have used in many of our previous calculations[16,21,41,42] and for the available experiments.[5,16,39,40] Here, by the DFT model we mean not only the GGA used, but also the parameters that affects the convergence of the DFT calculations, such as the number of metal layers used to model the surface and the basis set. The comparison is timely, because a very accurate representation of the DFT data in a global PES can now be obtained with the CRP method[35] used here, so that discrepancies between theory and experiment can no longer be attributed to possible deficiencies in the analytical representation of the PES. In addition, thanks to the development of a new symmetry adapted, fully pseudospectral wave-packet method[43] it is now possible to perform accurate 6D quantum dynamics calculations on scattering of H_2 from square surfaces for general expressions of the PES, such as obtained with the CRP method at a reasonable computational expense.

The model we use to describe the scattering of H_2 from Cu(100), the new potential-energy surface, the new wave-packet method, and some computational details are described in Secs. II A–II D. The comparison between theory and experiment for the new PES (PES5) and the previous PES (PES4) is discussed in Sec. III A for reaction, and in Sec. III B for rovibrationally elastic and inelastic scattering. Conclusions and possible future directions are discussed in Sec. IV.

II. METHOD

A. Model

In the model we use to study reactive scattering of H_2 from Cu(100), essentially two approximations are used. The first approximation is that we freeze the positions of the surface Cu atoms to their ideal lattice values, thereby neglecting energy transfer to and from the phonons. In the dynamics calculations discussed below, the motion in the remaining six, molecular degrees of freedom will be treated essentially exactly, using quantum mechanics. The coordinates used are shown in Fig. 1. Briefly, Z describes the distance of the molecule to the surface, X and Y are the center-of-mass coordinates of the molecule describing its motion parallel to the surface, r is the H–H distance, and θ and ϕ are the polar and azimuthal angles describing the orientation of the molecular axis. The second approximation is that we assume that the Born–Oppenheimer approximation holds and that the reaction takes place on the lowest, ground electronic state PES. The validity of both assumptions is discussed in Refs. 29–31.

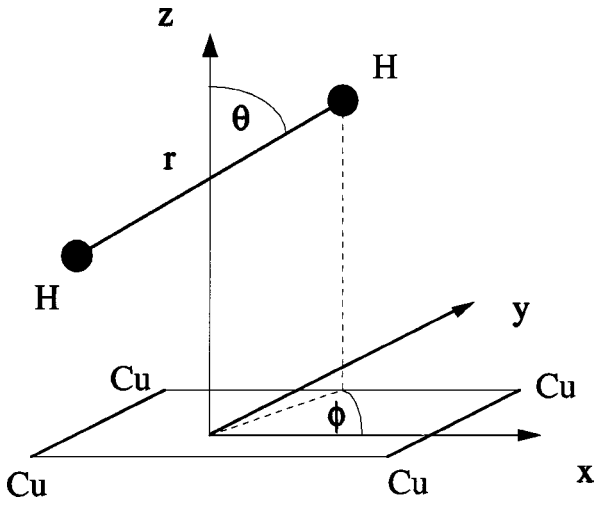

FIG. 1. Coordinate system used for studying reactive scattering of H_2 from Cu(100).

B. Potential-energy surfaces: PES4 and PES5

Both PES4 and PES5, which describe the interactions of the H atoms with one another and with the Cu(100) surface, are based on DFT calculations employing the same basis set and additional parameters relevant to the DFT calculations. The DFT calculations are described in detail in Refs. 20, 21, and 44; here, only a brief overview is given.

The DFT calculations were performed using the program BAND.[45,46] The program can solve the Kohn–Sham equations[47,48] for a periodic system, in our case a semi-infinite slab with translational symmetry in two directions. In the calculations, electronic densities were first calculated self-consistently using the local-density approximation (LDA).[49] Next, the exchange-correlation energy is obtained at the GGA level by combining the Becke correction[24] for the exchange energy and the Perdew correction[25] for the correlation energy, both corrections being computed from the self-consistent LDA density.

The calculations used a two-layer slab for the copper surface, employing the experimental Cu bulk lattice constant, $a=4.824a_0$.[50] A (2×2) overlayer of hydrogen molecules was used. The basis set consists of one Slater-type orbital and one numerical atomic orbital for all valence functions (H $1s$, Cu $3d$, and $4s$) and additional $2p$ and $4p$ polarization functions on H and Cu, respectively. The Cu atoms in the first layer have a frozen core up to $3p$, and those in the second layer up to $3d$. Full details of the basis set are given in Refs. 44 and 21. The accint parameter, which determines the accuracy of the real-space integration, was set to 4.0, and the *k*-space parameter, which governs the number of integration points in the surface Brillouin zone, was set to 5.

Due to previous computational constraints, the DFT data on which PES4 and PES5 are based were not fully converged. As discussed more fully in Ref. 21, the convergence errors due to the use of a small basis set and the use of a limited number of copper layers were both estimated to be approximately 0.1 eV, but because convergence tests showed these errors to be of opposite sign, it was estimated that the DFT results were converged to within 0.1 eV of the GGA limit.

The DFT data were fitted to an expansion in 14 symmetry-adapted functions of X, Y, θ, and ϕ in PES4. The fit was based on the DFT data obtained for 14 two-dimensional cuts in r and Z, computed for H_2 being above the top, hollow, and bridge high-symmetry sites in different orientations (for a detailed description, see Ref. 21). Because no data were included for intermediate surface sites, and because only spherical harmonics $Y_{jm_j}(\theta,\phi)$ with m_j even were employed in the expansion, PES4 does not describe the effect that the molecule-surface interaction is changed if H_2 is rotated by 180° in ϕ, if the molecule is not above one of the three high-symmetry sites and $\theta\neq90°$. PES4 is expected to provide a reasonably accurate description of the molecule-surface interaction above the three high-symmetry sites, but could overestimate or underestimate the anisotropy of the PES above these sites because spherical harmonics were included in the expansion up to fourth order ($j=4$) only. Above the low-symmetry sites, PES4 should be less accurate.

PES5[36] was fitted using the CRP method.[35] Briefly, the 6D PES V_{6D} is written as

$$V_{6D}(X,Y,Z,r,\theta,\phi) = I_{6D}(X,Y,Z,r,\theta,\phi) + V_{3D}(X_A,Y_A,Z_A) + V_{3D}(X_B,Y_B,Z_B). \quad (1)$$

The idea behind Eq. (1) is to eliminate the greater part of the corrugation and of the anisotropy from the expression to be fitted [which becomes I_{6D} with the use of Eq. (1)] by first subtracting the previously fitted interaction V_{3D} of two isolated hydrogen atoms [labeled A and B in Eq. (1)] from the DFT energies to be described by V_{6D}. Full details of the CRP method are provided in Ref. 35. The calculation of I_{6D} in PES5 was based on the DFT data obtained for 15 two-dimensional cuts in r and Z for H_2 above the three high-symmetry sites and one additional low-symmetry site (halfway between the top and hollow sites), in different orientations. Full details are presented in Ref. 36.

Figure 2 shows the dependence of PES5 on r and Z for the three high-symmetry sites and H_2 in its most favorable orientation parallel to the surface, and for an additional low-symmetry site where H_2 is in between the bridge and hollow site and assumes a tilted orientation. Even though the latter geometry was not included in the DFT calculations on which PES5 was based, PES5 correctly reproduces a previous finding of Kratzer *et al.*[51] that a very low barrier (0.51 eV) is obtained for this site, with H_2 in a tilted orientation. However, we still obtain the lowest barrier for the bridge-to-hollow configuration (0.50 eV), whereas Kratzer *et al.* obtained the lowest barrier for the low-symmetry site (the difference was, however, reported to be only 0.03 eV).[51] The barrier heights obtained for the hollow-to-bridge and top-to-bridge configurations also shown in Fig. 2 were 0.59 and 0.63 eV, respectively. For the three high-symmetry site configurations shown in Fig. 2, with H_2 parallel to the surface and $\phi=0$, PES4 and PES5 are essentially the same. However, PES5 also yields a correct description of the molecule-

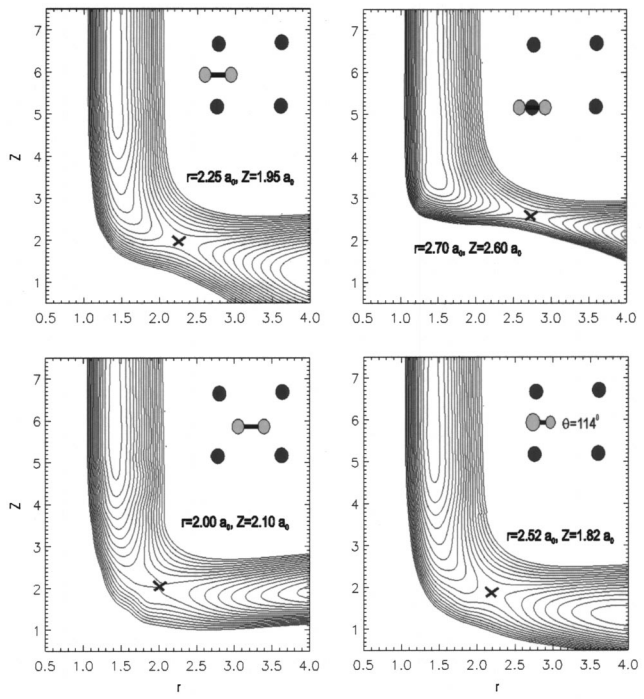

FIG. 2. Two-dimensional cuts through PES5 are shown for dissociation of H_2 on Cu(100). In all four cases, the dissociation geometry (X, Y, and ϕ) is indicated in the inset in the upper-right corner, and the barrier geometry is indicated by a cross and described by its r and Z values. Three of the four configurations are for H_2 parallel to the surface above the bridge, top, and hollow high-symmetry sites. The fourth configuration is described by $X=0.96a_0$, $Y=2.41a_0$, $\theta=114°$, and $\phi=0°$. Contours are shown for $E=-0.1$ to 1.1 eV with spacings of 0.06 eV, and $E=0$ eV corresponding to the minimum of the H_2 potential in the gas phase.

surface interaction for H_2 above low-symmetry sites (see Ref. 36), also correctly describing the effect that the molecule-surface interaction is changed if H_2 is rotated by 180° in ϕ. Furthermore, a comparison of the interpolated PES5 with DFT data for points not used in the basis for interpolation shows that PES5 describes the DFT data quite accurately; at such points, the maximum errors are below 20 meV in the entrance channel and below 40 meV in the intermediate barrier region.[36]

C. Dynamical method

The Hamiltonian describing the motion of the H atoms interacting with a static Cu(100) surface is

$$-\frac{1}{2M}\left(\frac{\partial^2}{\partial X^2}+\frac{\partial^2}{\partial Y^2}+\frac{\partial^2}{\partial Z^2}\right)-\frac{1}{2\mu}\frac{\partial^2}{\partial r^2}+H_{\mathrm{rot}}+V_{6\mathrm{D}}(X,Y,Z,r,\theta,\phi). \quad (2)$$

In Eq. (2), M and μ are the mass and the reduced mass of H_2, respectively, H_{rot} is the Hamiltonian describing the rotation of the molecule, and $V_{6\mathrm{D}}$ is the PES describing the interaction of the H atoms with one another and with the surface. Atomic units are used in Eq. (2) and below.

To obtain reaction probabilities, we solve the time-dependent Schrödinger equation

$$\psi^{vjm_j}(Q;t)=\exp(-iHt)\psi^{vjm_j}(Q;t=0) \quad (3)$$

using the time-dependent wave-packet (TDWP) method.[52] In Eq. (3), Q denotes the set of coordinates used. Full details of the TDWP methods employed for PES4 and PES5 can be found elsewhere.[43,53] Here, we only give a brief outline.

The TDWP calculations are started from a real initial wave function $\psi^{vjm_j}(Q;t=0)$ which contains the product of a Gaussian wave packet describing motion in Z and a rovibrational wave function describing the initial vibrational and rotational state (vjm_j) of H_2. To describe motion at normal incidence and to normalize the wave function with respect to X and Y, the initial wave function also contains a factor $1/\sqrt{A}$, where A is the area of the surface unit cell. In both cases (for both PESs), a representation of the wave function is used that is adapted to the symmetry of the surface unit cell and the inversion symmetry of the molecule.[43,53] The wave function is propagated in time using the absorbing boundary-conditions evolution operator expression due to Mandelshtam and Taylor.[54] During the propagation, time-dependent overlaps of the wave function with asymptotic gas phase (rovibrational diffraction) states of H_2 are obtained. Time-to-energy Fourier transforms of these overlaps are used to obtain S-matrix elements $S_{vjm_j\rightarrow v'j'm'_jnm}(E)$ using the scattering amplitude formalism of Balint-Kurti *et al.*[55,56] and Mowrey and Kroes;[57] here, n and m are the diffraction quantum numbers.

From the S-matrix elements, probabilities for scattering to final rovibrational diffraction states are obtained as

$$P_{vjm_j\rightarrow v'j'm'_jnm}(E)=|S_{vjm_j\rightarrow v'j'm'_jnm}(E)|^2. \quad (4)$$

Initial state-resolved reaction probabilities R_{vjm_j} can be computed using

$$R_{vjm_j}(E)=1-\sum_{v'j'm'_jnm}P_{vjm_j\rightarrow v'j'm'_jnm}(E). \quad (5)$$

Degeneracy-averaged reaction probabilities R_{vj} can be obtained by degeneracy averaging the R_{vjm_j} over m_j. Similarly, degeneracy-averaged probabilities for rovibrationally inelastic scattering $P_{vj\rightarrow v'j'}$ can be obtained by summing the $P_{vjm_j\rightarrow v'j'm'_jnm}$ over m'_j, n, and m and degeneracy averaging over m_j.

The calculations employing PES4 and PES5 are done using different implementations of the TDWP method. In both implementations, an expansion in symmetry-adapted rotation-diffraction functions is used as the primary representation. The calculations on PES4 are done using a close-coupling wave-packet formalism, employing a method which has been called the symmetry-adapted wave-packet (SAWP) method.[53,58] This method expresses the potential operator in a potential coupling matrix containing matrix elements between rotation-diffraction states, taking advantage of the fact that this matrix is sparse for PES4, which is expanded in only 14 symmetry-adapted rotation-diffraction functions.

The use of the SAWP method would be prohibitively expensive for a more general fit expression of the PES, such as obtained when employing the CRP method (PES5). Therefore, some of us have recently developed a method[43] that still takes advantage of the symmetry associated with the surface

TABLE I. Values of the parameters used in the wave-packet calculations with the SAWP and the SAPS method. Note: in the SAPS calculations, the surface lattice constant used is the experimental value reported in Ref. 50. In the SAWP calculations, a slightly different, older experimental value was used.

		PES4 (SAWP)	PES5 (SAPS)		
Parameter	Description	$v=1$, $j=1$	$v=0$, $j=0$	$v=1$, $j=0$	$v=1$, $j=1$
N_r	Number of grid points in r	40		40	
Δr	Spacing of r grid (a_0)	0.15		0.15	
r_{start}	Start value of grid in r (a_0)	0.522		0.522	
N_Z	Number of grid points in Z	90		96	
ΔZ	Spacing of Z grid (a_0)	0.14		0.15	
Z_{start}	Start value of grid in Z (a_0)	−1.0		0.0	
N_Z^{sp}	Number of specular grid points	144		128	
$J_{\max}$	Maximum j value in basis set	21	28		29
O_{diff}	Maximum diffraction order	11		⋯	
$nm_{\max}$	Maximum diffraction state	⋯		13	
t_{tot}	Total propagation time (a.u.)	60 000	45 000	52 000	
Δt_{an}	Time step for analyses (a.u.)	40.0	20.0	40.0	
a	Surface lattice constant (a_0)	4.822		4.824	
$V_{\max}$	Cutoff potential (eV)	16.0	10.0	5.5	
$K_{\max}$	Cutoff kinetic operators (eV)		5.5		
γ_r	Strength-damping function in r		0.2		
$r_{\min}^{\text{opt}}$	Start optical V of r grid (a_0)	4.00		3.82	
$r_{\max}^{\text{opt}}$	End optical V of r grid (a_0)		6.37		
γ_Z	Strength-damping function in Z		0.05		
$Z_{\min}^{\text{opt}}$	Start optical V of Z grid (a_0)	6.84		9.00	
$Z_{\max}^{\text{opt}}$	End optical V of Z grid (a_0)	11.46		14.25	
$\gamma_{Z,sp}$	Strength-damping function specular grid		0.05		
$Z_{\min,sp}^{\text{opt}}$	Start optical V specular grid (a_0)	13.84		13.05	
$Z_{\max,\text{opt}}^{sp}$	End optical V specular grid (a_0)	19.02		18.45	
Z_0	Center initial wave packet (a_0)	10.2		11.0	
E_{range}	Normal-incidence energy range initial wave packet (eV)	0.06–0.20	0.3–1.15	0.1–1.15	
Z_∞	Location analysis line (a_0)	6.84		8.55	

unit cell and of the molecule, but uses the discrete variable representation (DVR) to compute the action of the potential-energy operator on the wave function. This method, which has been called the symmetry-adapted pseudospectral (SAPS) method, uses cosine and sine transforms between the momentum and coordinate representations of the parts of the symmetry-adapted wave function describing diffraction. This is done in combination with a symmetry-adapted version of the Gauss–Legendre–Fourier transform algorithm for the rotations that was originally developed by Corey and Lemoine,[59] to transform between the symmetry-adapted wave function in the finite basis representation (FBR) and in the DVR representation, in a fully pseudospectral approach. Full details of this method are presented in Ref. 43.

D. Computational details

The parameters used in the TDWP calculations for PES4[16,21] and PES5 are given in Table I. The meaning of most of the parameters is self-evident; here we only discuss those of which the meaning may be less obvious.

For reasons discussed in Ref. 53, the wave-packet calculations are performed employing a projection operator formalism,[60] in which the rovibrationally elastic scattering channel is kept on a separate grid in Z (called the ''specular grid'') throughout the calculation. The number of points used for this grid is indicated by N_Z^{sp}, and the specular grid starts at the same value of Z and has the same spacing as the Z grid in the ''6D grid.''

The SAWP calculations employ a diamond-shaped grid of diffraction states in momentum space,[53] and O_{diff} defines the maximum value of $|n|+|m|$, where n and m are the diffraction quantum numbers. In contrast, the SAPS method[43] uses a square grid, $nm_{\max}$ defining the maximum value of n and m.

In the propagation using the ABC evolution operator method,[54] the wave function is damped at the edges of the grid by damping the modified Chebyshev polynomials using an exponential function of $\rho=r$ or Z, defined by

$$\hat{\gamma}_\rho=\gamma_\rho[(\rho-\rho_{\min}^{\text{opt}})/(\rho_{\max}^{\text{opt}}-\rho_{\min}^{\text{opt}})]^2, \quad \rho_{\min}^{\text{opt}}\leqslant\rho\leqslant\rho_{\max}^{\text{opt}}. \tag{6}$$

This damping procedure emulates the action of an energy-dependent optical potential.[54] In Table I, values of the parameters of Eq. (6) are provided for Z (for the large grid and the specular grid) as well as r.

The tests conducted indicated the convergence of reaction and scattering probabilities presented here to within 1% with respect to basis sizes and propagation times.

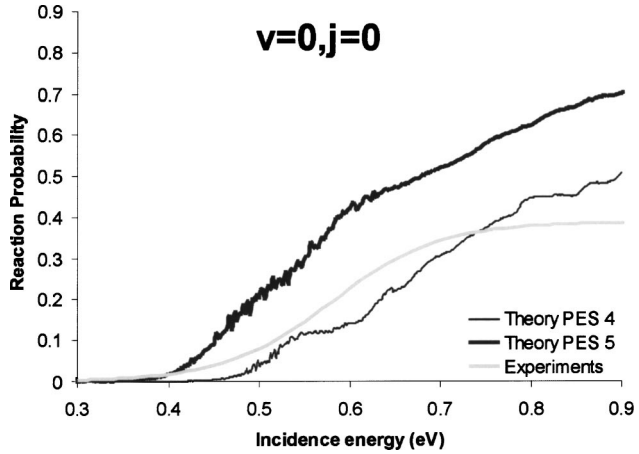

FIG. 3. The reaction probability of ($v=0$, $j=0$) H_2 is shown as a function of the collision energy for normal incidence. Computational results for PES4 (Ref. 21) and PES5 are compared with the experimentally fitted reaction probability of ($v=0$) H_2 (Ref. 40).

III. RESULTS AND DISCUSSION

A. Dissociative chemisorption

Dissociative chemisorption probabilities computed for PES5 are compared with previous results for PES4[21] and with experimental results[40] in Fig. 3 for ($v=0$, $j=0$) H_2, and in Fig. 4 for ($v=1$, $j=0$) H_2. The reaction probability curve for PES5 appears to be shifted towards lower E_i relative to the previous results for PES4, for reaction of ($v=0$, $j=0$) H_2 (Fig. 3). The energy shift is lower at low E_i (about 0.07 eV) than at higher E_i (up to 0.17 eV). A similar energy shift of the reaction probability curve is observed when comparing the results for ($v=1$, $j=0$) H_2 (Fig. 4), although the energy shift is somewhat lower on average for $v=1$. The reaction probability curves computed for PES4 were in excellent agreement with the experiment, but due to the energy shift the agreement between the reaction probabilities computed for PES5 and the experimental fits is clearly not as good.

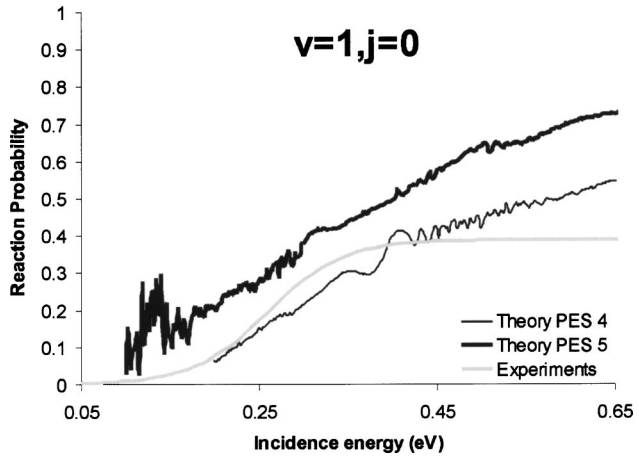

FIG. 4. The reaction probability of ($v=1$, $j=0$) H_2 is shown as a function of the collision energy for normal incidence. Computational results for PES4 (Ref. 21) and PES5 are compared with the experimentally fitted reaction probability of ($v=1$) H_2 (Ref. 40).

A major difference between PES4 and PES5 is that PES5 also gives an accurate description of the molecule-surface interaction for H_2 impacting on low-symmetry sites,[36] as obtained with DFT. In particular, PES4 is not able to describe the effect that the molecule can lower its energy at some of these sites by tilting away from the orientation parallel to the surface for certain values of ϕ, because the fit expression used imposed that $V(\theta,\phi)=V(\theta,\phi+180°)$ also for $\theta\neq 90°$. At the intermediate sites, this should lead to values of the molecule-surface interaction potential that are too high for many orientations. In addition, plots of PES4 and PES5 not presented here show that, at intermediate sites, PES4 systematically overestimates the molecule-surface interaction also for orientations of H_2 parallel to the surface, when comparing with the DFT data not used in the fit. As a result of these effects, the total zero-point energy of the molecule at the bridge site barrier should also be too high for PES4. Consequently, the reaction probabilities computed with PES4 would be expected to be too low due to the limitations of and the symmetry constraints imposed by the fitting method.[21] This explains why the reaction probabilities computed with PES5 are shifted towards lower energies relative to those computed with PES4. Plots of the polar and azimuthal anisotropies of PES4 and PES5 not presented here show that the discrepancies between the computed reaction probabilities cannot be a consequence of an inaccurate representation of the potential anisotropy of PES4 at the high-symmetry sites; at the barrier geometries at these sites, both PES4 and PES5 describe the angular dependence of the DFT data quite well up to molecule-surface interaction energies of 1 eV.

Comparing the results for the reaction obtained with the more accurately fitted PES to the experiment, it could perhaps be viewed as disappointing to observe that the agreement with experiment, which was quite good for PES4, has detoriated now that a much more accurate method[35] was used to represent the DFT data in a PES. However, one should keep in mind that studies of gas phase reactions have revealed that barrier heights for gas phase reactions computed by the DFT/GGA method are usually accurate to within 0.1–0.2 eV only, and that the DFT/GGA method usually underestimates the barrier height.[61,62] Furthermore, there is also considerable uncertainty in the accuracy of the experimentally fitted reaction probabilities, for reasons discussed in depth in Ref. 53. Nevertheless, we have gone back to our original DFT calculations, to see how the computed results might change for an accurately fitted PES based on fully converged DFT data obtained using the Becke–Perdew GGA.[24,25] Preliminary results of single-point calculations for geometries where H_2 is close to the barrier and above the high-symmetry sites suggest that the DFT energies may go up by as much as 0.2 eV if a basis set of TZ2P (triple zeta +2 polarization functions) quality is used in conjunction with the use of five copper layers. This could well lead to reaction probability curves that would be shifted to higher energies compared to experiment, but this is yet uncertain because the locations of the barriers may also change. Further research (the calculation of a completely new set of fully converged DFT data) is required to establish how good the agreement for reaction would be between experiment and 6D

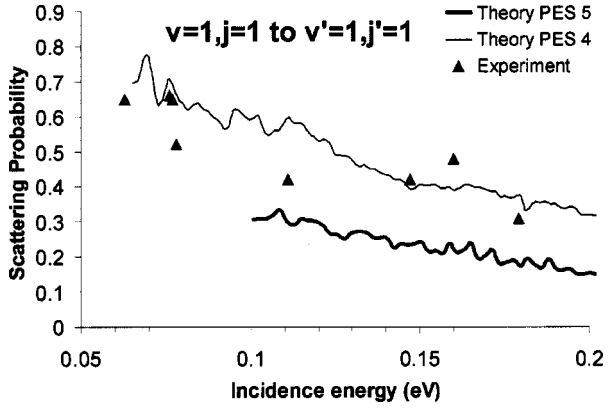

FIG. 5. The probability for rovibrationally elastic scattering of H_2 from the $(v=1, j=1)$ initial state is shown as a function of the collision energy for normal incidence. Computational results for PES4 (Ref. 16) and PES5 are compared with experimental results (Ref. 16).

quantum dynamics based on an accurately fitted set of fully converged DFT data calculated at the Becke–Perdew GGA[24,25] level.

B. Rovibrationally (in)elastic scattering

Probabilities for scattering of H_2 from the $(v=1, j=1)$ initial state that were computed with PES5 are compared with the results for PES4[16] and with experimental results[16] in Fig. 5 for rovibrationally elastic scattering and in Fig. 6 for rotational excitation to the $(v=1, j=3)$ state. The results obtained for PES4 for $E_i \geqslant 100$ meV come from Ref. 16. The results obtained for PES4 at lower E_i have not yet been published.

The probability of rovibrationally elastic scattering obtained with PES5 is smaller than that obtained with PES4 over the entire range of E_i for which results were obtained for PES5 ($E_i \geqslant 100$ meV) (Fig. 5). As a result, the agreement for rovibrationally elastic scattering between experiment and theory, which was good for PES4, is no longer good for PES5; the computed probabilities for rovibrationally elastic scattering are too low. The lowering of this probability in going from PES4 to PES5 does not appear to be due to

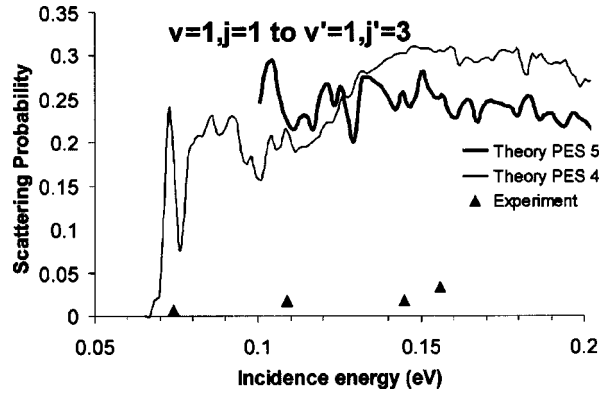

FIG. 6. The probability for rotational excitation of H_2 from the $(v=1, j=1)$ to the $(v=1, j=3)$ state is shown as a function of the collision energy for normal incidence. Computational results for PES4 (Ref. 16) and PES5 are compared with experimental results (Ref. 16).

TABLE II. Probabilities for rovibrationally inelastic scattering of H_2 from the $(v=1, j=1)$ initial state, at normal incidence.

Final state	$v=0, j=5$	$v=0, j=7$
Experiment, $E_i=74$ meV (Ref. 16)	9×10^{-3}	5×10^{-4}
Theory, PES4, $E_i=74$ meV	60×10^{-3}	24×10^{-4}
Theory, PES4, $E_i=100$ meV (Ref. 16)	61×10^{-3}	22×10^{-4}
Theory, PES5, $E_i=100$ meV	72×10^{-3}	104×10^{-4}

increased competition with rotational excitation to the $j=3$ state, the probability for this process being more or less equal for PES4 and PES5 (Fig. 6). Rather, the difference appears to be largely due to increased competition with reaction. The reaction probability obtained with PES5 for $(v=1, j=0)$ H_2 is larger than that obtained with PES4 by 0.10–0.15 for $0.1 \leqslant E_i \leqslant 0.2$ eV (Fig. 4) and similar results were obtained for the $(v=1, j=1)$ state (results not shown here).

As already mentioned, the probabilities for rotational excitation to the $(v=1, j=3)$ state computed for PES4 and PES5 are similar for $0.1 \leqslant E_i \leqslant 0.2$ eV (Fig. 6). The computed probabilities for rotational excitation are much higher than the experimental values, indicating that the scattered molecules experience too much anisotropy in their interaction with the surface for these collision energies, with the potential models studied.

Probabilities for vibrational deexcitation accompanied by rotational excitation obtained with theory and experiment are compared in Table II. The theoretical values for PES4 computed for $E_i=100$ meV overestimate the experimental values obtained for the somewhat lower $E_i=74$ meV by factors of 5–6 for both the $(v=0, j=5)$ and the $(v=0, j=7)$ final states. The new results obtained for PES4 at the experimental value of E_i (74 meV) suggest that this result is not a consequence of the somewhat higher value of E_i (100 meV) used in the original calculations.[16] The comparison between the probabilities obtained with PES4 and PES5 at the latter value of E_i show that the agreement between experiment and theory, which was already quite bad for PES4, only detoriates further with the use of PES5.

The detoriated agreement between experiment and theory obtained for PES5 for scattering as well as reaction and the results of preliminary DFT calculations performed using a larger basis set and more Cu layers (see Sec. III A above) have caused us to reconsider the explanation we previously gave of the discrepancies between theory and experiment for scattering. The reaction probabilities computed with PES5 are too high compared to experiment, and the preliminary DFT calculations suggest that this is probably due to the barriers being too low in PES5 because the DFT calculations were not fully converged. If an accurately fitted PES were to be based on converged DFT data, the reaction probability curves would shift to higher energies and the rovibrationally elastic scattering of $(v=1, j=1)$ H_2 (Fig. 5) would be less affected by competition with reaction. This could lead to better agreement with experiment for this channel. Furthermore, because such a new PES would be more repulsive, the molecules that scatter nonreactively would be less able to come close to the barrier, where they are able to experience

the large anisotropies that promote rotational excitation. As a result, the probability for rotational excitation should become lower than that obtained with PES5, and the agreement with experiment would also improve for this channel (see Fig. 6). We would also expect to see smaller probabilities for transitions to the $(v=0, j=5)$ and the $(v=0, j=7)$ states, for the same reason, and again this would improve the agreement with the experiment (Table II).

Additional sources of error in the calculations on scattering include the neglect of phonons and of electron-hole pair excitations. As previously discussed in more detail,[16] we do not believe that inclusion of these in our model would have a big effect on the theoretical results. Furthermore, as should be clear from the above results, the first place to look for improvement is the DFT potential; this should now also be based on well-converged DFT calculations, such that the experimental reaction probabilities are hopefully reproduced with the same level of accuracy as obtained for PES4, but now also for an accurately fitted PES that correctly describes the molecule-surface interaction also above low-symmetry sites.

IV. CONCLUSIONS AND FUTURE

We have performed six-dimensional quantum dynamical calculations on the dissociative chemisorption of $(v=0, 1, j=0)$ H_2 on Cu(100), and on rovibrationally (in)elastic scattering of $(v=1, j=1)$ H_2 from Cu(100). The dynamics results were obtained using a new PES (PES5), which was based on DFT calculations using a slab representation of the adsorbate-substrate system and the Becke–Perdew GGA to the exchange-correlation energy. The difference with previous calculations, which were based on PES4, is that a very accurate method (the corrugation-reducing procedure) was used to represent the DFT data in a global PES (PES5). The accuracy of the fitting method used is such that any discrepancies observed between theory and experiment can only be due to the dynamical model (Born–Oppenheimer approximation, frozen surface) and/or the DFT model used (GGA and parameters determining the convergence of the DFT calculations).

With the new, more accurately fitted PES5 the agreement between the dynamics results and experimental results for reaction is not as good as it was for PES4. More specifically, the theoretical reaction probability curves for $(v=0, j=0)$ and $(v=1, j=0)$ H_2 are shifted to lower energies compared to the experimentally fitted curves for $(v=0)$ and $(v=1)$ H_2. Preliminary results of single-point DFT calculations for geometries where H_2 is close to the barrier and above the high-symmetry sites suggest that the DFT energies will increase if a basis set of higher quality is used in conjunction with more copper layers. This may well lead to improved agreement between experiment and theory for a PES that is both based on well-converged DFT data and accurately fitted PES. The previous very good agreement between experimental reaction probabilities and the theoretical results obtained for PES4 was fortuitous; it was apparently based on a cancellation of errors due to the imperfect convergence of the DFT calculations on the one hand and the use of a less-accurate fitting method on the other hand.

Likewise, the agreement between theory and experiment for rovibrationally (in)elastic scattering from the $(v=1, j=1)$ initial H_2 state detoriates when going from PES4 to PES5. The theoretical probability for rovibrationally elastic scattering obtained with PES5 is too low compared to experiment, probably due to too much competition with reaction. The theoretical probability for rotational excitation to the $(v=1, j=3)$ state is much too high compared with experiment, as it was for PES4. For both processes, better agreement would be expected for an accurately fitted PES based on well-converged DFT data at the Becke–Perdew level. Because such a PES should be more repulsive, there should be less competition of reaction with rovibrationally elastic scattering, and rotationally inelastic scattering should become diminished because the scattering molecules would be less able to sample the highly anisotropic regions of the PES near the higher barriers.

The tools for producing an accurately fitted PES are now in place; for this, the corrugation-reducing procedure[35] can be used, as well as a modified Shepard interpolation procedure first developed for gas phase reactions but recently tested on reactive and inelastic scattering of H_2 from Pt(111).[63] Furthermore, whereas the DFT calculations alluded to in Sec. III A, which would use a TZ2P quality basis set in conjunction with five copper layers, are not computationally inexpensive, they are quite doable, and they would yield a highly converged PES. Such DFT calculations can be done while obtaining results for different GGA's (such as Becke–Perdew,[24,25] PW91,[26] and RPBE[64]) at the same time, at a relatively small extra computational expense. In addition, the availablity of a new symmetry-adapted pseudospectral wave-packet method now makes it possible to perform accurate 6D quantum dynamics calculations on reactive scattering of H_2 from surfaces for general expressions of the PES at a reasonable computational expense, for square surfaces, and it should be possible to generalize this method to rectangular and hexagonal surfaces. In short, it should now be possible to obtain 6D quantum dynamics results for reaction and scattering based on accurately fitted, well-converged DFT data, for several GGA's, and to compare these results to the many experimental results which are available for reactive and inelastic scattering of H_2 from metal surfaces, for the system studied here as well as the other systems. This way, one might also hope to evaluate which GGA's work best for describing reactive scattering of H_2 from metal surfaces, and, presumably, for reactive interactions of other molecules with metal surfaces.

ACKNOWLEDGMENTS

This research was supported by a CW/NWO program grant and by the National Computing Facilities foundation. We are grateful to D. Lemoine for helping us implement his FBR/DVR scheme for treating rotational motion into our new SAPS code, and for numerous useful discussions.

[1] C. T. Rettner, H. A. Michelsen, and D. J. Auerbach, J. Chem. Phys. **102**, 4625 (1995).
[2] C. T. Rettner, D. J. Auerbach, and H. A. Michelsen, Phys. Rev. Lett. **68**, 1164 (1992).

[3] H. A. Michelsen, C. T. Rettner, D. J. Auerbach, and R. N. Zare, J. Chem. Phys. **98**, 8294 (1993).
[4] B. E. Hayden and C. L. A. Lamont, Phys. Rev. Lett. **63**, 1823 (1989).
[5] G. Anger, A. Winkler, and K. D. Rendulic, Surf. Sci. **220**, 1 (1989).
[6] K. D. Rendulic, G. Anger, and A. Winkler, Surf. Sci. **208**, 404 (1989).
[7] A. C. Luntz, J. K. Brown, and M. D. Williams, J. Chem. Phys. **93**, 5240 (1990).
[8] M. Gostein and G. O. Sitz, J. Chem. Phys. **106**, 7378 (1997).
[9] D. Wetzig, R. Dopheide, M. Rutkowski, R. David, and H. Zacharias, Phys. Rev. Lett. **76**, 463 (1996).
[10] H. Hou, S. J. Gulding, C. T. Rettner, A. M. Wodtke, and D. J. Auerbach, Science **277**, 80 (1997).
[11] A. Hodgson, J. Moryl, P. Traversaro, and H. Zhao, Nature (London) **356**, 501 (1992).
[12] C. T. Rettner, D. J. Auerbach, and H. A. Michelsen, Phys. Rev. Lett. **68**, 2547 (1992).
[13] M. Gostein, H. Parhikhteh, and G. O. Sitz, Phys. Rev. Lett. **75**, 342 (1995).
[14] A. Hodgson, P. Samson, A. Wight, and C. Cottrell, Phys. Rev. Lett. **78**, 963 (1997).
[15] M. Gostein, E. Watts, and G. O. Sitz, Phys. Rev. Lett. **79**, 2891 (1997).
[16] E. Watts, G. O. Sitz, D. A. McCormack *et al.*, J. Chem. Phys. **114**, 495 (2001).
[17] G. J. Kroes, A. Gross, E. J. Baerends, M. Scheffler, and D. A. McCormack, Acc. Chem. Res. **35**, 193 (2002).
[18] B. Hammer, M. Scheffler, K. W. Jacobsen, and J. K. Nørskov, Phys. Rev. Lett. **73**, 1400 (1994).
[19] S. Wilke and M. Scheffler, Phys. Rev. B **53**, 4926 (1996).
[20] G. Wiesenekker, G. J. Kroes, and E. J. Baerends, J. Chem. Phys. **104**, 7344 (1996).
[21] D. A. McCormack, G. J. Kroes, R. A. Olsen, J. A. Groeneveld, J. N. P. van Stralen, E. J. Baerends, and R. C. Mowrey, Faraday Discuss. **117**, 109 (2000).
[22] R. A. Olsen, G. J. Kroes, and E. J. Baerends, J. Chem. Phys. **111**, 11155 (1999).
[23] W. Dong and J. Hafner, Phys. Rev. B **56**, 15396 (1997).
[24] A. D. Becke, Phys. Rev. A **38**, 3098 (1988).
[25] J. P. Perdew, Phys. Rev. B **33**, 8822 (1986).
[26] J. P. Perdew, J. A. Chevary, S. H. Vosko, K. A. Jackson, M. R. Pederson, D. J. Singh, and C. Fiolhais, Phys. Rev. B **46**, 6671 (1992).
[27] G. te Velde and E. J. Baerends, Chem. Phys. **177**, 399 (1993).
[28] J. Neugebauer and M. Scheffler, Phys. Rev. B **46**, 16067 (1992).
[29] G. R. Darling and S. Holloway, Rep. Prog. Phys. **58**, 1595 (1995).
[30] A. Gross, Surf. Sci. Rep. **32**, 291 (1998).
[31] G. J. Kroes, Prog. Surf. Sci. **60**, 1 (1999).
[32] E. Pijper, G. J. Kroes, R. A. Olsen, and E. J. Baerends, J. Chem. Phys. **117**, 5885 (2002).
[33] A. Eichler, J. Hafner, A. Gross, and M. Scheffler, Phys. Rev. B **59**, 13297 (1999).
[34] H. F. Busnengo, E. Pijper, M. F. Somers, G. J. Kroes, A. Salin, R. A. Olsen, D. Lemoine, and W. Dong, Chem. Phys. Lett. **356**, 515 (2002).
[35] H. F. Busnengo, A. Salin, and W. Dong, J. Chem. Phys. **112**, 7641 (2000).
[36] R. A. Olsen, H. F. Busnengo, A. Salin, M. F. Somers, G. J. Kroes, and E. J. Baerends, J. Chem. Phys. **116**, 3841 (2002).
[37] H. F. Busnengo, C. Crespos, W. Dong, J. C. Rayez, and A. Salin, J. Chem. Phys. **116**, 9005 (2002).
[38] S. M. Kingma, M. F. Somers, E. Pijper, G. J. Kroes, R. A. Olsen, and E. J. Baerends, J. Chem. Phys. **118**, 4190 (2003).
[39] G. Comsa and R. David, Surf. Sci. **117**, 77 (1982).
[40] H. A. Michelsen and D. J. Auerbach, J. Chem. Phys. **94**, 7502 (1991).
[41] D. A. McCormack, G. J. Kroes, R. A. Olsen, J. A. Groeneveld, J. N. P. van Stralen, E. J. Baerends, and R. C. Mowrey, Chem. Phys. Lett. **328**, 317 (2000).
[42] M. F. Somers, D. A. McCormack, G. J. Kroes, R. A. Olsen, E. J. Baerends, and R. C. Mowrey, J. Chem. Phys. **117**, 6673 (2002).
[43] M. F. Somers, D. Lemoine, and G. J. Kroes, Chem. Phys. (in press).
[44] G. Wiesenekker, G. J. Kroes, E. J. Baerends, and R. C. Mowrey, J. Chem. Phys. **102**, 3873 (1995).
[45] G. te Velde and E. J. Baerends, Phys. Rev. B **44**, 7888 (1991).
[46] G. te Velde and E. J. Baerends, J. Comput. Phys. **99**, 84 (1992).
[47] P. Hohenberg and W. Kohn, Phys. Rev. **136**, B864 (1964).
[48] W. Kohn and L. J. Sham, Phys. Rev. **140**, A1133 (1965).
[49] S. H. Vosko, L. Wilk, and M. Nusair, Can. J. Phys. **58**, 1200 (1980).
[50] C. Kittel, *Introduction to Solid State Physics* (Wiley, New York, 1986).
[51] P. Kratzer, B. Hammer, and J. K. Nørskov, Surf. Sci. **359**, 45 (1996).
[52] R. Kosloff, J. Phys. Chem. **92**, 2087 (1988).
[53] G. J. Kroes, E. J. Baerends, and R. C. Mowrey, J. Chem. Phys. **107**, 3309 (1997).
[54] V. A. Mandelshtam and H. S. Taylor, J. Chem. Phys. **103**, 2903 (1995).
[55] G. G. Balint-Kurti, R. N. Dixon, and C. C. Marston, J. Chem. Soc., Faraday Trans. **86**, 1741 (1990).
[56] G. G. Balint-Kurti, R. N. Dixon, and C. C. Marston, Int. Rev. Phys. Chem. **11**, 317 (1992).
[57] R. C. Mowrey and G. J. Kroes, J. Chem. Phys. **103**, 1216 (1995).
[58] G. J. Kroes, J. G. Snijders, and R. C. Mowrey, J. Chem. Phys. **103**, 5121 (1995).
[59] G. C. Corey and D. Lemoine, J. Chem. Phys. **97**, 4115 (1992).
[60] D. Neuhauser and M. Baer, J. Chem. Phys. **91**, 4651 (1989).
[61] M. T. Nguyen, S. Creve, and L. G. Vanquickenborne, J. Phys. Chem. **100**, 18422 (1996).
[62] J. Baker, M. Muir, and J. Andzelm, J. Chem. Phys. **102**, 2063 (1995).
[63] C. Crespos, M. A. Collins, E. Pijper, and G. J. Kroes, J. Chem. Phys. **120**, 2392 (2004).
[64] B. Hammer, L. B. Hansen, and J. K. Nørskov, Phys. Rev. B **59**, 7413 (1999).